Anisotropy of the ferromagnetic L1 0 phase in the Mn-Al-C alloys induced by high-pressure spark plasma sintering

Muriel Tyrman, Smail Ahmim, Alexandre Pasko, Victor H. Etgens, Frederic Mazaleyrat, Simon Quetel-Weben, Loïc Perrière, Ivan Guillot

Anisotropy of the ferromagnetic $L1_0$ phase in the Mn-Al-C alloys induced by high-pressure spark plasma sintering

Muriel Tyrman,[1, a)] Smail Ahmim,[1] Alexandre Pasko,[1] Victor Etgens,[1] Frédéric Mazaleyrat,[1] Simon Quetel-Weben,[2] Loïc Perrière,[2] and Ivan Guillot[2]
[1)] *SATIE, ENS Paris-Saclay, CNRS, 61 av President Wilson, 94230 Cachan, France*
[2)] *ICMPE, CNRS, UPEC, 2-8 rue Henri Dunant, 94320 Thiais, France*

The metastable τ-phase of MnAl equi-atomic compound belongs to a family of ferromagnetic alloys with $L1_0$ crystal structure. Stabilization of the phase by adding 2 at. % using manganese carbide ($Mn_{23}C_6$) enhances the magnetization in relation with the increase in lattice volume. It is thus a promising candidate for rare-earth-free permanent magnets. Coercivity of Mn-Al-C alloys being still weak, there is an interest to see to which extend sintering/transformation of the ϵ-phase by Spark Plasma Sintering (SPS) can increase the coercivity and the anisotropy. The structural and the magnetic properties were studied for samples sintered at 550 °C under uniaxial pressure of 100, 200, 300 and 400 MPa. Coercivity, remanence and anistotropy appears with the sintering pressure. The high pressure applied while sintering produces preferential orientation of the flake-shaped grains which influences the remanence.

I. INTRODUCTION

In the field of rare-earth free magnets, MnAl alloys are promising candidates with magnetic properties potentially filling the gap between hard ferrites and Nd-Fe-B[3]. These candidates are particularly interesting because they are light, do not contain rare-earth or strategic elements, and are more resistant at high temperature than Nd-Fe-B. It is then an innovative material for greener electrical vehicles[5,6]. MnAl alloys ferromagnetic tetragonal τ-phase belongs to the $L1_0$ family of ordered crystal structures. This τ-phase is metastable, it is obtained after annealing the quenched hexagonal ϵ-phase existing at high temperature with Mn in excess. Since ϵ-phase and τ-phase are metastable, addition of 2 at. % of C is needed to stabilize the τ-phase and to increase the coercivity[2]. For these reasons, the composition $Mn_{54}Al_{44}C_2$ is chosen to obtain ϵ-phase by melt-spinning[7–10].
In our previous studies, the C was added by several routes to optimize the synthesis : (i) pieces of graphite, (ii) graphite powder, and (iii) manganese carbide ($Mn_{23}C_6$)[1]. The use of $Mn_{23}C_6$ as a C source results in more homogeneous samples with better magnetic properties. Indeed, the addition of C increases the lattice volume, and as 1a and 1d Mn sites of the lattice are antiferromagnetically coupled, the increase of lattice volume decrease the magnetic coupling between those sites, resulting in higher magnetization.
Despite a high anisotropy field around 5 T, the coercivity of Mn-Al-C alloys remains weak. To improve the coercivity, as quenched Mn-Al-C alloys were mechanically milled at low temperature (around 77 K) in the ϵ-phase[4,11,12]. Then, the obtained powder was sintered by *Spark Plasma Sintering* (SPS) process in a tungsten carbide mold. The transformation from ϵ-phase to τ-phase is performed under a stress in order to influence the anisotropy of the samples. Compared to a graphite mold, the tungsten carbide mold is used to sinter at high pressure at lower temperature. Thin powder of the alloys was sintered by SPS at 400 MPa at temperatures from 500 to 600 °C[4,13]. We showed in our results that the powder was mechanically activated by the milling process, giving more equilibrium β and γ_2 non-magnetic phases, but high densities of the samples. However, we noticed that 25 % of β-phase in the sample increases the coercivity for about 40 % for an alloy sintered at 550 °C and 400 MPa. This study compared the magnetic properties of the samples as a function of τ, β and γ_2 phases proportions, for different sintering temperatures. A small anisotropy was obtained, and the coercivity was higher in the sintering pressure direction with a lower magnetization in this direction, compared to the magnetization measured perpendicularly to the direction of pressure.
From the previous results, the chosen sintering temperature was 550 °C and in this paper, the crystallographic and magnetic properties as a function of the sintering pressure are presented.

II. EXPERIMENTAL DETAILS

$Mn_{54}Al_{44}C_2$ alloys were obtained by melting pure manganese, aluminum and manganese carbide ($Mn_{23}C_6$) in a cold crucible induction furnace. Ribbons of pure ϵ-phase were produced by melt-spinning. A powder was obtained after cryogenic mechanical milling of the ribbons. The powder was then sintered under argon by *Spark Plasma Sintering* (the sample is heated by a pulsed electric current) in 8 mm tungsten carbide mold. Sintering is then done at much higher pressure than with a graphite mold[9,13] and therefore at lower temperature to obtain high densities of the pellets and to avoid precipitation of β-phase (Mn-rich cubic phase) and γ_2-phase (Al-rich trigonal phase)[14]. Structural properties of all samples

[a)] Muriel.Tyrman@satie.ens-cachan.fr

(powder in the ϵ-phase and all pellets) were determined by X-ray diffraction (XRD) using a Bruker D2 Phaser diffractometer equipped with a LinxEye Linear detector in Co Kα radiation. The magnetic measurements were performed at room temperature using a LakeShore 7400 vibrating sample magnetometer (VSM) in the three directions of cubes of around 3 mm edge cut in the pellets : one direction is parallel to the sintering pressure direction, and two directions are perpendicular to the sintering pressure direction. The measurements were limited to 1.9 T by the VSM used here, but we checked that the same coercive fields were obtained for a 9 T max field.

III. RESULTS AND DISCUSSION

A. Spark plasma sintering

The Table I present the preparation conditions of the samples with the labels used in paper[4] (S for sintered solid, F for fine milling). All samples were sintered at 550 °C for pressure from 100 to 400 MPa. The Archimedes' principle was used to determine the density of samples. Then, the relative density was calculated from the XRD data. The results show that, as expected, the density of all samples increases with sintering pressure and temperature[4].

TABLE I. Preparation conditions and relative density of samples.

Sample	Treatment (MPa)	Density (%)
SF100	100	87
SF200	200	89
SF300	300	96
SF400	400	98

B. X-ray diffraction

The lattice parameters and the phase constitution were determined by using the Rietveld refinement software MAUD[15]. The phase diagram[14] shows two equilibrium phases depending on the proportions of Mn and Al atoms : β-phase and γ_2-phase. The ϵ phase is stable at high temperature but can be obtained in non-equilibrium conditions. The τ metastable phase is obtained after annealing the quenched ϵ-phase.
From X-ray diffraction, the as prepared powder is a pure ϵ-phase. As shown in Fig.1 and Table II, the material is almost fully in τ-phase, but the sintering process produces the precipitation of few % of β-phase. A higher proportion of τ-phase for the same sintering temperature and pressure is obtained by decreasing the milling velocity compared to ref.[4]. The crystallites size is around 60 nm.

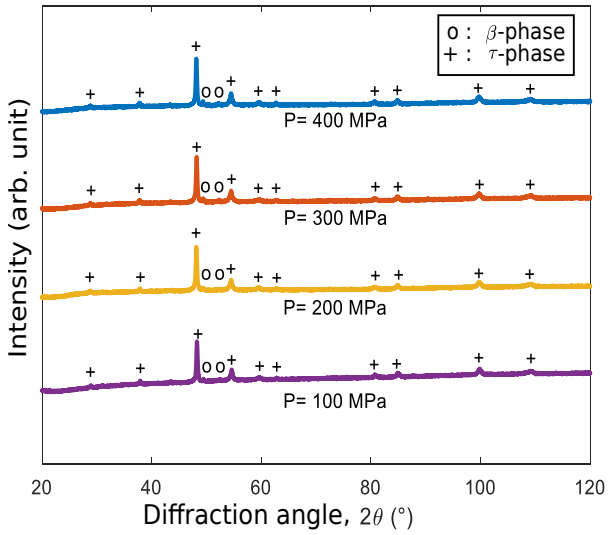

FIG. 1. XRD patterns of the samples sintered at 100, 200, 300 and 400 MPa.

TABLE II. Phase fraction determined by XRD.

Sample	τ-phase (%)	β-phase (%)
SF100	94	6
SF200	95	5
SF300	92	8
SF400	95	5

C. Magnetic properties

Measurements in both of the perpendicular give the same magnetic properties, so only two directions of the measurements are presented : parallel and perpendicular to the pressure axis.
The results are presented in Fig. 2. The hysteresis loops recorded in both direction overlaps for a pressure of 100 MPa but the parallel loop is significantly below the perpendicular one for higher pressures. The magnetic properties, i.e. coercivity $\mu_0 H_c$, remanence J_r and magnetization $J_{1.9}$ at 1.9 T, are presented on Fig.3 and Fig. 4 in both orientation, parallel and perpendicular. The samples are not saturated under the field of 1.9 T (about 70% of the saturation after our previous work[9]) but the aim of this study is only to compare the samples processed in different conditions of pressure.

The increase of $\mu_0 H_c$ and J_r with pressure, and the gap between the two directions are presented on Fig.3 and Fig.4. This gap is clearly increasing with pressure. The fact that anisotropy appears with high sintering pressure,

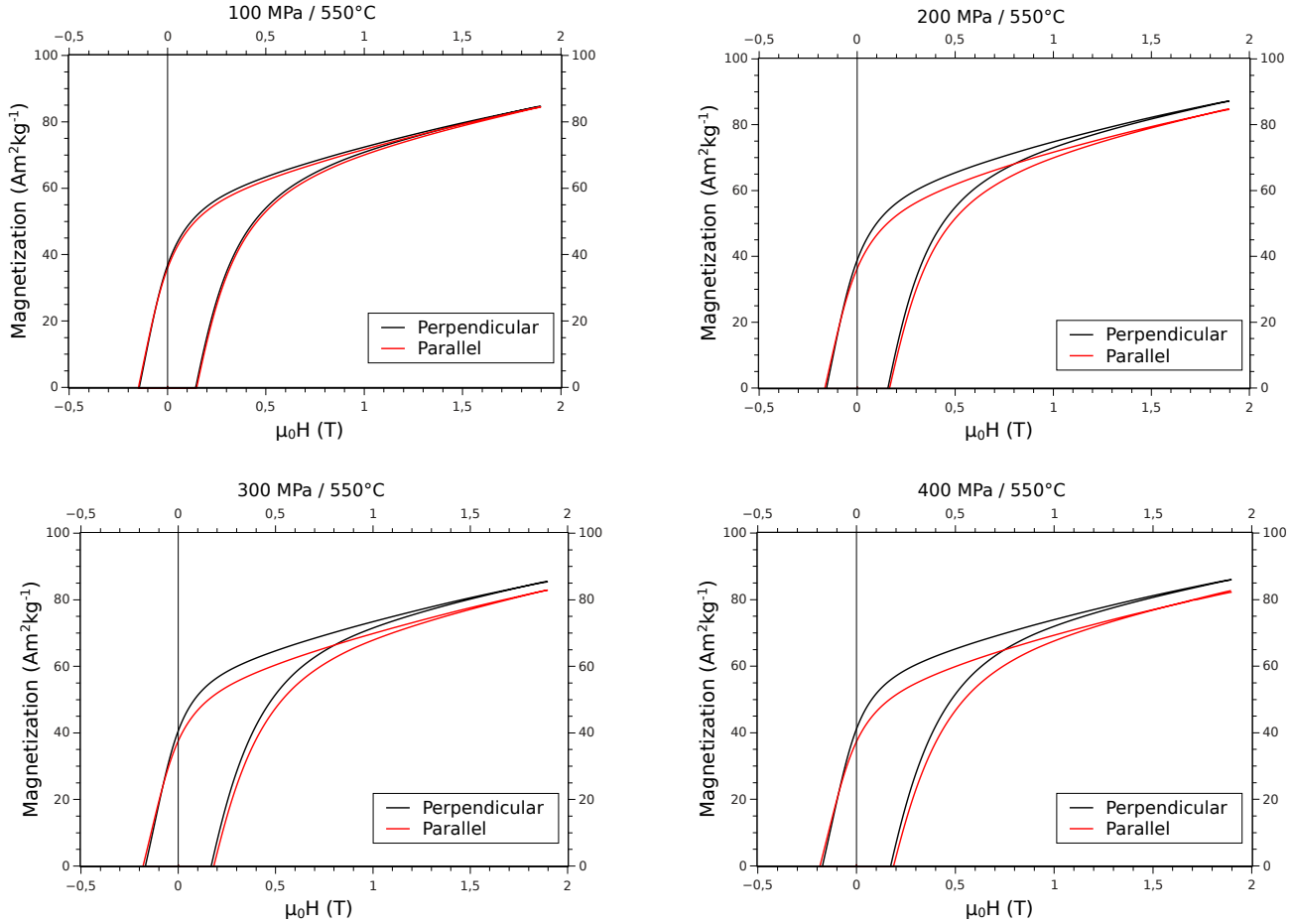

FIG. 2. Magnetization ($\mathrm{A\,m^2\,kg^{-1}}$) versus $\mu_0 H_c$ (T) of the samples sintered at 550 °C and 100, 200, 300 and 400 MPa, measured parallel and perpendicular to the sintering pressure direction.

is in line with results from the extrusion method which is performed directly in the τ-phase[16], and the anisotropy result is in line too with the results from hot-deformed method[17].

In Fig. 4, the gap between the measurements of $\mu_0 H_c$ in both directions is similarly increasing with the pressure. For comparison, the coercivity was measured for a sample sintered from the same batch, but annealed in a classical furnace. This reference sample was transformed without stress and was single τ-phase. These results suggest that $\mu_0 H_c$ does not depend on the quantity of β-phase, but only on the stress applied while sintering. Until a pressure of 300 MPa, there is a linear relation between the pressure and $\mu_0 H_c$ (Fig. 4). To explain this result, we propose the hypothesis that texturation appears, which means that there is a development of variants with the c-axis oriented perpendicularly to the stress direction. However, the X-ray diffraction performed on 2 perpendicular faces of the cubes doesn't allow us to conclude on the texture yet. Texture was neither observed by electron backscatter diffraction (EBSD)[4]. However, M_r is very sensitive to texture, so a weak preferential orientation may explains the increase in M_r measured perpendicularly to stress and the decrease when measured parallel to stress.

To clarify this result, a Scanning Electron Microscopy (SEM) image of the sample sintered at 550 °C under vertical uniaxial pressure of 400 MPa is presented in Fig. 5. The material is composed of flat flakes of around 100-200 μm long and 20 μm wide. The flakes are composed of crystallites of around 60 nm (X-ray diffraction). At 400 MPa, preferential orientation in the horizontal plane of the flakes is clearly observed. The pressure thus introduces mesoscopic shape anisotropy with a higher demagnetizing field parallel to pressure, in agreement with the lower magnetization in this direction (Fig. 2).

IV. CONCLUSION

After quenching the ϵ-phase by melt-spinning and after ball milling at low temperature of the ribbons, bulk $Mn_{54}Al_{44}C_2$ permanent magnets were produced. Using a tungsten carbide mold allows to decrease the temperature and to increase pressure while sintering, in order to control the volume fraction of the ferromagnetic τ-phase.

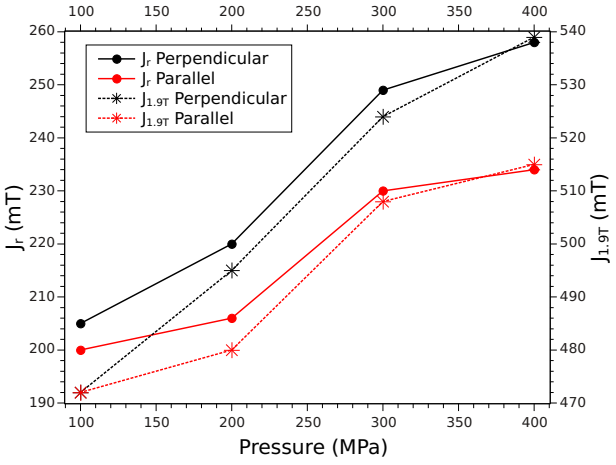

FIG. 3. Curves of residual magnetization (left axis) and magnetization at 1.9 T (right axis) versus sintering pressure measured parallel and perpendicular to the pressure axis.

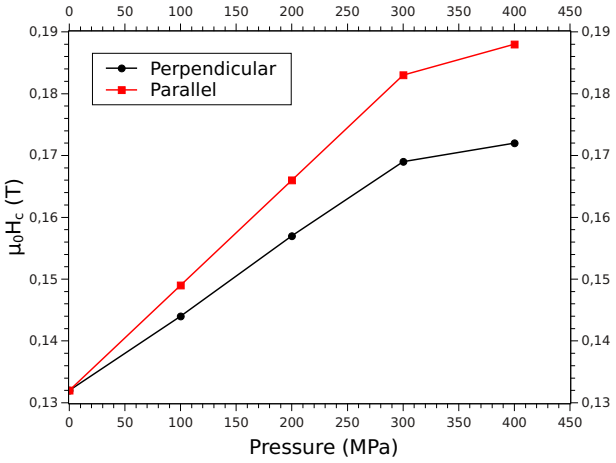

FIG. 4. Curves of coercivity versus sintering pressure measured parallel and perpendicular to the sintering pressure direction.

We have observed that the Mn-Al-C samples sintered at 550 °C under a uniaxial pressure of 100 to 400 MPa exhibit a noticeable anisotropy of magnetic properties and strong dependence of the coercivity on stress.
This effect should be explained rather by the shape anisotropy related to the global in plane orientation of flakes produced by the stress applied during sintering than a texture effect since XRD patterns exhibit the features of an isotropic material for all samples. However, according to Stoner and Wohlfarth, H_c and M_r both increase when measuring $M(H)$ within the easy axis contrarily to the present results. So, if the mesoscopic perpendicular shape anisotropy is prevalent on the remanence, it is not in principle affecting the coercivity because the crystallites are much smaller than the grains. Consequently there may be another kind of microscopic parallel anisotropy induced by stress, either due to small texture or residual strain.

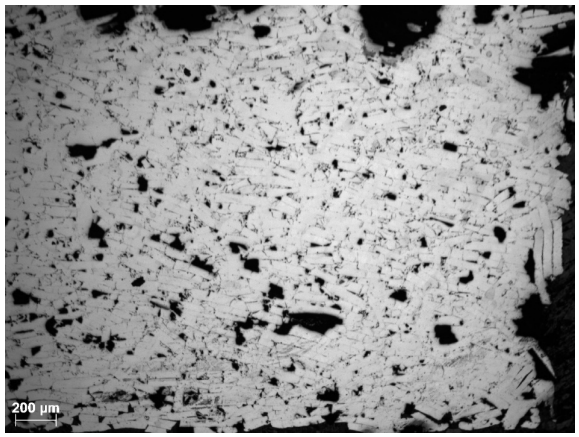

FIG. 5. SEM image of the sample sintered at 550 °C under vertical uniaxial pressure of 400 MPa.

ACKNOWLEDGMENTS

M. Tyrman thanks L'Oréal-UNESCO *For Women In Science* for financial support (FRANCE L'Oréal-UNESCO *For Women In Science* 2017 fellowship).

[1] M. Tyrman, A. Pasko, L. Perrière, V. Etgens, O. Isnard, and F. Mazaleyrat, IEEE Transactions on Magnetics **53**, 2101406 (2017).
[2] T. Ohtani, N. Kato, S. Kojima, K. Kojima, Y. Sakamoto, I. Konno, M. Tsukahara, and T. Kubo, IEEE Transactions on Magnetics **13**, 1328 (1977).
[3] J. Coey, Journal of Physics: Condensed Matter **26**, 064211 (2014).
[4] M. Tyrman, S. Quetel-Weben, A. Pasko, L. Perrière, I. Guillot, V. Etgens, and F. Mazaleyrat, IEEE Transactions on Magnetics **53**, 2101505 (2017).
[5] J. Coey, Scripta Materialia **67**, 524 (2012).
[6] M. Kramer, R. McCallum, I. Anderson, and S. Constantinides, Jom **64**, 752 (2012).
[7] E. Fazakas, L. Varga, and F. Mazaleyrat, Journal of Alloys and Compounds **434**, 611 (2007).
[8] A. Pasko, F. Mazaleyrat, M. LoBue, E. Fazakas, and L. Varga, in *EPJ Web of Conferences*, Vol. 40 (EDP Sciences, 2013) p. 06008.
[9] A. Pasko, F. Mazaleyrat, L. K. Varga, P. S. Stamenov, and J. M. D. Coey, IEEE Transactions on Magnetics **50**, 1 (2014).
[10] P. Saravanan, V. Vinod, M. Černík, A. Selvapriya, D. Chakravarty, and S. Kamat, Journal of Magnetism and Magnetic Materials **374**, 427 (2015).
[11] A. Koch, P. Hokkeling, M. vd Steeg, and K. De Vos, Journal of Applied Physics **31**, S75 (1960).
[12] R. McCurrie, J. Rickman, P. Dunk, and D. Hawkridge, IEEE Transactions on Magnetics **14**, 682 (1978).
[13] A. Pasko, M. Lobue, E. Fazakas, L. Varga, and F. Mazaleyrat, Journal of Physics: Condensed Matter **26**, 064203 (2014).
[14] A. Shukla and A. D. Pelton, Journal of phase equilibria and diffusion **30**, 28 (2009).
[15] L. Lutterotti, Acta Crystallogr., Sect. A: Found. Crystallogr **56**, S54 (2000).
[16] Y. Sakamoto, A. Ibata, S. Kojima, and T. Ohtani, IEEE Transactions on Magnetics **16**, 1056 (1980).
[17] R. Madugundo and G. C. Hadjipanayis, Journal of Applied Physics **119**, 013904 (2016).